

SOLUTION OF THE DISPERSION RELATION FOR MAGNETIZED MULTI-FLUID PLASMA USING PDRF: A CASE STUDY OF SOLAR WIND

¹A. M. Nura and ²A. J. Ado

¹Department of Physics, Bayero University, Kano.

¹ Department of Physics, Yusuf Maitama Sule University, Kano, Nigeria.

²Government Secondary School Bomo (Senior), Zaria, Kaduna State

Abstract

The solar wind is mostly populated by collisionless, anisotropic and inhomogeneous plasma. Wave propagation in plasma can be studied using fluid or kinetic model. In this work the fluid model is applied in solving Plasma dispersion relation for magnetized multi-fluid plasma by employing PDRF code (Plasma Dispersion Relation Fluid-version). The dispersion relation of the solar wind plasma was solved by varying plasma β - value for ions for $k_z \ll k_\perp$. The threshold values of the growth rate were found for $\beta_\perp < \beta_\parallel$ and $\beta_\perp > \beta_\parallel$. As β_\perp decrease below β_\parallel following a criteria that: $P_\parallel - P_\perp > B_0^2/\mu_0$, the growth rate increases indicating fire hose instability. At $\beta_\parallel = \beta_\perp$, the growth rate was found to be very small indicating transit-time damping. When β_\perp increase above β_\parallel , the growth rate increased indicating mirror instability.

Keywords: Plasma physics, Solar wind, Dispersion relation, Multi-Fluid, Waves, Matrix eigenvalue, Instabilities.

1.0 Introduction

It is difficult to be able to characterize a plasma system without considering its wave behaviour. In doing so, solving the dispersion relation is one of the basic problems encountered in that aspect of plasma physics and which is of practical interest [1].

Dispersion relation is the function that relates the frequency of the wave in the plasma and its wave vector [2]. Usually, the dispersion relation is obtained from the determinant of the dielectric tensors of the wave equations.

Ronmark [3] used the kinetic code WHAMP (Waves in Homogeneous Anisotropic Multicomponent Magnetized Plasma) to solve linear analytic dispersion equations of waves in magnetized plasma. It includes a number of species with different density, mass, temperature and drift parameters for anisotropic Maxwellian distribution [3, 4, 5]. Bret presented a Mathematica fluid code for magnetized parallel beam plasmas which allowed for the symbolic calculation of the (3x3) dielectric tensor of an electron-beam plasma system in the fluid approximation. The calculation was detailed for a cold relativistic electron beam entering a cold magnetized plasma, and arbitrarily oriented wave vector [1]. However, it is difficult to generalize such treatment to include arbitrary number of fluid species with good convergence or to obtain all the solutions of a given system. But with the introduction of the Plasma Dispersion Relation Fluid-version (PDRF) by Xie [6], it is possible to solve dispersion relation for magnetized multi-fluid plasmas for arbitrary number of species with good convergence including anisotropy, relativistic beam and weak inhomogeneity effects. This made it easy to investigate wave properties in astrophysical, space, laser, and laboratory plasmas.

Pressure or temperature anisotropy is an important characteristic of collisionless plasma in a strong magnetic field [7] and may develop in the sun, solar wind and planetary magnetospheres, etc. for example gyrotropic pressure of $P_\perp > P_\parallel$ and $P_\parallel > P_\perp$ tends to develop in the Earth's magnetosheath and magnetotail, respectively [8, 9]. In the magnetohydrodynamic theory, sufficiently large pressure anisotropy of $P_\perp > P_\parallel$ or $P_\parallel > P_\perp$ may lead to the mirror and fire-hose type instability in a homogeneous magnetized plasma respectively. Instabilities in this regime is considered as velocity space instability at low frequencies ($\omega \ll \omega_{ci}$) as well as at long wavelengths ($\lambda \gg Q_i = v_T/\omega_{ci}$) where ω_{ci} is ion cyclotron frequency, Q_i is the ratio of thermal velocity to ion cyclotron frequency of the plasma. It occurs in a high β plasma and are caused by anisotropic pressure, where β is the ratio of plasma kinetic pressure to magnetic pressure [10]. Such instabilities could be treated using

Correspondence Author: Nura A.M., Email: nuraa2622@buk.edu.ng, Tel: +2347063517772

Transactions of the Nigerian Association of Mathematical Physics Volume 9, (March and May, 2019), 119 – 124

MHD equations with anisotropic pressure or kinetic equations. Hasegawa [10] used the kinetic equations to show some significant differences from the results of the MHD equations by introducing a dielectric tensor obtained from the kinetic equations for the hydromagnetic limit: $k_{\perp} v_T / \omega_{ci} \sim \omega / \omega_{ci} \ll 1$, where k_{\perp} is the wave vector perpendicular to the external magnetic field. In the expressions the effects of wave-particle resonance anisotropic distribution, and existence of relative drift between different species are retained to be used for a study of instabilities.

In this work, we used the general dispersion relation solver PDRF to execute the task of obtaining solutions of dispersion relation

$$D(\omega, k) = 0$$

for solar wind. The solution is obtained for when and where the k or ω are complex. The imaginary part of k or ω determines if the oscillations become damped or growing (depending on the sign of the imaginary part). From a mathematical point of view, with perturbation analysis we can study whether an initial perturbation causes undamped oscillations, or whether oscillations are damped or are growing [11]. Here, the firehose and mirror instabilities threshold growth rates were investigated for $\beta_{\parallel} > \beta_{\perp}$ and $\beta_{\parallel} < \beta_{\perp}$ with $k_{\parallel} < k_{\perp}$ respectively. Where, k_{\parallel} is the wave vector parallel to the magnetic field, k_{\perp} is the wave vector perpendicular to the magnetic field, β_{\parallel} and β_{\perp} are the plasma beta-values parallel and perpendicular to the magnetic field respectively.

2.0 Theoretical Frame Work

We ignored all temperature gradient effects in the cold multi-fluid plasma, flow velocity of the fluid component j is taken as $v_{j0} = (v_{j0x}, v_{j0y}, v_{j0z})$ in an external static magnetic field $B_0 = (0, 0, B_0)$. The species densities are considered to be locally inhomogeneous, with $\nabla n_{j0} / n_0 = (\epsilon_{njx}, \epsilon_{n jy}, 0) = constant$. The wave vector is assumed to be $k = (k_x, 0, k_z) = (k \sin \theta, 0, k \cos \theta)$. We use the fluid equations to develop a full dispersion relation matrix and instead of directly solving for its determinant such as that of Swanson [2] or analytical or numerical treatment such as in Stix [12], Ronnmark [3, 4] and Bret [1], we treated it as a matrix eigenvalue problem [6].

The governing equations are the fluid equations:

$$\frac{\partial n_j}{\partial t} = -\nabla \cdot (n_j \mathbf{v}_j) \tag{1a}$$

$$\frac{\partial \mathbf{u}_j}{\partial t} = -v_j \cdot \nabla \mathbf{u}_j + \frac{q_j}{m_j} (\mathbf{E} + \mathbf{v}_j \times \mathbf{B}) - \frac{\nabla P_j}{\rho_j} - \sum_i (\mathbf{u}_i - \mathbf{u}_j) v_{ij} \tag{1b}$$

$$\frac{\partial \mathbf{E}}{\partial t} = c^2 \nabla \times \mathbf{B} - \mathbf{J} / \epsilon_0 \tag{1c}$$

$$\frac{\partial \mathbf{B}}{\partial t} = -\nabla \times \mathbf{E} \tag{1d}$$

where $\mathbf{u}_j = \gamma_j \mathbf{v}_j$, and

$$\mathbf{J} = \sum_j q_j n_j \mathbf{v}_j \tag{2a}$$

$$\frac{d}{dt} (\mathbf{P}_{\parallel j} \rho_j^{-\gamma_{\parallel j}}) = 0 \tag{2b}$$

$$\frac{d}{dt} (\mathbf{P}_{\perp j} \rho_j^{-\gamma_{\perp j}}) = 0 \tag{2c}$$

where $\rho_j \equiv m_j n_j$, $c^2 = 1 / \mu_0 \epsilon_0$, $\gamma_j = (1 - v_j^2 / c^2)^{-1/2}$, and $\gamma_{\parallel j}$ and $\gamma_{\perp j}$ are the parallel and perpendicular adiabatic coefficients, respectively. $\mathbf{P}_{\parallel \perp} = n T_{\parallel \perp}$, $\mathbf{P} = P_{\parallel} \hat{\mathbf{b}} \hat{\mathbf{b}} + P_{\perp} (\mathbf{I} - \hat{\mathbf{b}} \hat{\mathbf{b}})$ is anisotropic pressure and $\hat{\mathbf{b}} = \mathbf{B} / B$. The anisotropy model can be reduced to that of Bret and Deutsch [13] by setting $\gamma_{\parallel j} = \gamma_{\perp j} = \gamma_{Tj}$. By further setting $T_{\perp j} = T_{\parallel j}$, we can recover the isotropic pressure case.

After linearizing, (1) becomes

$$\mathbf{J} = \sum_j q_j (n_{j0} v_{j1} + n_{j1} v_{j0}), \tag{3a}$$

$$P_{\parallel, \perp j1} = c_{\parallel, \perp j}^2 n_{j1}, \tag{3b}$$

where $c_{\parallel, \perp}^2 = \gamma_{\parallel, \perp} P_{\parallel, \perp j0} / \rho_{j0}$ and $P_{j0} = n_{j0} T_{j0}$

we note that

$$\nabla \cdot P_{j1} = (ik_x, 0, ik_z) \begin{vmatrix} P_{\perp j1} & 0 & \Delta_j B_{x1} \\ 0 & P_{\perp j1} & \Delta_j B_{y1} \\ \Delta_j B_{x1} & \Delta_j B_{y1} & P_{\parallel j1} \end{vmatrix}$$

where $\Delta_j = (P_{\parallel j0} - P_{\perp j0}) / B_0$ and $\beta_{\parallel, \perp j} = 2 \mu_0 P_{\parallel, \perp j} / B_0^2$. The off-diagonal terms coming from the tensor rotation from \hat{b}_0 to \hat{b} are related to energy exchange and are important for the anisotropic instabilities. An incorrect treatment or ignoring these off-diagonal terms can cause loss of the firehose and other unstable anisotropic modes.

The program is designed to use $method = 1$, $method = 2$, $method = 3$ and $method = 4$. When the program is set to $method = 1$, it will generate all the linear harmonic wave solutions of the system without any convergence difficulty. By setting the program to $method = 2$, it will plot dispersion curves $\omega_{r,i}$ versus k for various values of θ . If the program is set to $method = 3$, it will plot dispersion curves $\omega_{r,i}$ versus θ for various values of k . When the program is set to $method = 4$, it will plot curves $\omega_{r,i}$ versus k_x and k_z for range of values of k_x and k_z . The input file `pdrf.in` has the following structure.

<i>qs</i>	<i>ms</i>	<i>ns</i>	<i>vsx</i>	<i>vsy</i>	<i>vsz</i>	<i>csz</i>	<i>csp</i>	<i>epsnjx</i>	<i>epsnjz</i>
-1.0	1.0	10.0	0.0	0.0	0.0	0.0	0.0	0.0	0.0
1.0	1836.0	10.0	0.0	0.0	0.0	0.0	0.0	0.0	0.0

where *qs* is charge of species, *ms* is the mass of species, *ns* is the density of species, *vsx*, *vsy* and *vsz* are speed of species in x, y and z directions respectively, *csz* and *csp* are sound speeds in parallel and perpendicular direction to the magnetic field respectively. *epsnjx* and *epsnjz* are density gradient per unit density of species.

3.1 Procedure

Firstly, the parallel and perpendicular sound speeds, *csz* and *csp*, parallel and perpendicular pressures for solar wind plasma were calculated for $\beta_{\parallel i} = 0.5$, $\beta_{\perp i} \leq \beta_{\parallel i}$ and $\beta_{\perp i} \geq \beta_{\parallel i}$ respectively while $\beta_{\parallel,Le}$ were set to zero. The MATLAB program code was modified to suit the various basic parameters for solar wind plasma in Table 1. The ratio of parallel to perpendicular wave vector was set to $k_z/k_{\perp} = 0.01$ to indicate oblique propagation.

Table 1. Basic plasma parameters for magnetospheric plasmas [16].

Plasma parameter	Solar Wind at 1A.U	Low-latitude Boundary layer	Plasma Mantle	Tail Lobe	Plasma Sheet	Plasmasphere	Polar Wind (low altitude)	Topside Ionosphere
Number Density $n_i (cm^{-3})$	10	10	1	10^{-2}	1	10^3	0.1	10^4
Ion Temperature T_i (K)	10^5	5×10^6	10^6	10^5	5×10^7	10^5	10^5	10^3
Plasma flow speed v (kms^{-1})	400	200	150	40	10	10	20	0.1
Main Chemical Composition	H^+, He^{++}	H^+, He^{++}	H^+, He^{++}	H^+, He^+, O^+, N^+	$H^+, He^+, O^+, N^+, He^{++}$	H^+, He^+, O^+, N^+	H^+, He^+, O^+, N^+	H^+, He^+, O^+, N^+
Magnetic Field B (nT)	10	40	25	25	10	10^3	10^4	10^5
Scale Length L (km)	10^8	10^4	10^5	10^5	10^4	10^4	10^4	10^3
Mean free path (km)	10^9	10^{12}	10^{12}	10^{10}	10^{15}	10^7	10^{11}	10^2
Thermal ion gyroradius (km)	10^2	10^2	10^2	10^2	10^3	1	0.1	10^{-3}
Plasma beta β	0.5	1	0.5	10^{-4}	10	10^{-3}	10^{-9}	10^{-8}

Secondly, the input data file of the PDRF code was then modified to suit *csp*, *csz* and *ns* for the solar wind. The PDRF code was also modified to $rel = 0$ which reduce it to non relativistic case, with $m_i/m_e = 1836$ and $\gamma = 5/3$ for ideal gas [17]. The inputfile for solar wind is given below for $\beta_{\parallel i} = \beta_{\perp i} = 0.5$

<i>qs</i>	<i>ms</i>	<i>ns</i>	<i>vsx</i>	<i>vsy</i>	<i>vsz</i>	<i>csz</i>	<i>csp</i>	<i>epsnjx</i>	<i>epsnjz</i>
-1.0	1.0	10.0	0.0	0.0	0.0	0.0	0.0	0.0	0.0
1.0	1836.0	10.0	0.0	0.0	0.0	4.24e-1	4.24e-1	0.0	0.0

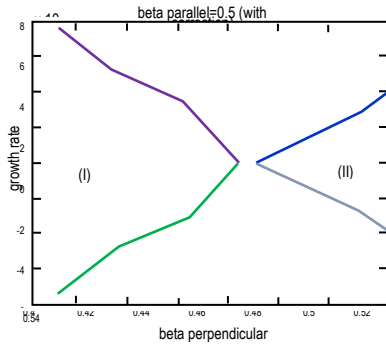
where, all parameters still maintain their usual meanings.

Thirdly, on the command window, a call to `pdrf` will generate all the linear harmonic wave solutions of the system without any convergence difficulty using $method = 1$.

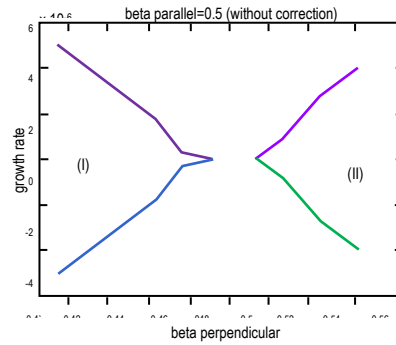
Fourthly, the threshold values of the complex part, ω_i of the solution were obtained for both with and without correction. Threshold values for the growth rate were plotted for $\beta_{\parallel} < \beta_{\perp}$ and $\beta_{\parallel} > \beta_{\perp}$.

4.0 Results and Discussion

The solutions of the dispersion relations of the solar wind plasma are given in forms of graphs. Figures 1.1(a-b) shows the graphs of growth rate against β_{\perp} for curves of (I) $\beta_{\perp i} < \beta_{\parallel i}$ and (II) $\beta_{\perp i} > \beta_{\parallel i}$ for constant value of $\beta_{\parallel i}$ (with correction and without correction) for firehose and mirror instability thresholds for the solar wind plasma.



1.1(a)

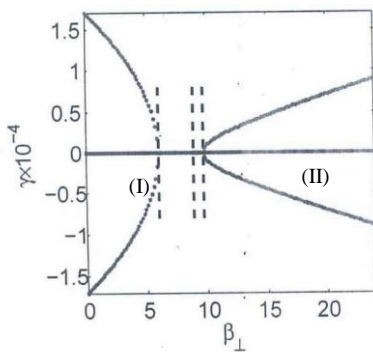


1.1(b)

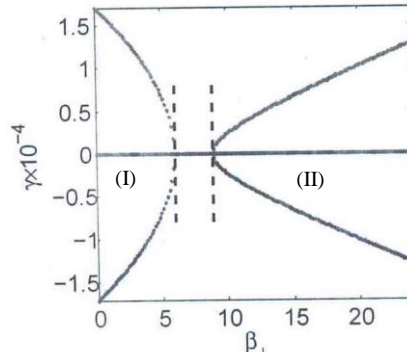
Fig. 1.1(a). The graph of growth rate against β_{\perp} for curves of (I) $\beta_{\perp i} < \beta_{\parallel i}$ and (II) $\beta_{\perp i} > \beta_{\parallel i}$ for constant value of $\beta_{\parallel i} = 0.5$ (with correction) for firehose and mirror instability thresholds respectively for the solar wind plasma, with $B_0 = 10nT, n_i = 10cm^{-3}$ and $\beta = 0.5$

Fig. 1.1(b). The graph of growth rate against β_{\perp} for curves of (I) $\beta_{\perp i} < \beta_{\parallel i}$ and (II) $\beta_{\perp i} > \beta_{\parallel i}$ for constant value of $\beta_{\parallel i} = 0.5$ (without correction) for firehose and mirror instability thresholds respectively for the solar wind plasma, with $B_0 = 10nT, n_i = 10cm^{-3}$ and $\beta = 0.5$

Figures 1.2(a-b) are the solutions of the test problem which was obtained and plotted.



1.2 (a)



1.2 (b)

Figure 1.2(a). (I) The firehose and (II) mirror instability thresholds for a test problem with correction for $\beta_{\parallel i} = 8$ and $\beta_{\parallel, \perp e} = 0$ by Xie [11]. The dots indicate theoretical prediction.

Figure 1.2(b). (I) Firehose and (II) mirror instability thresholds for a test problem without correction for $\beta_{\parallel i} = 8$ and $\beta_{\parallel, \perp e} = 0$ by Xie [11]. The dots indicates theoretical predictions

In Figures 1.1a and 1.1b the lowest value of the growth rate obtained was at a point where $\beta_{\parallel} = \beta_{\perp} = 0.5$ with a sound speed $c_{\parallel} = c_{\perp} = 4.24 \times 10^{-1}cms^{-1}$ and pressure of $P_{\parallel} = P_{\perp} = 1.98 \times 10^3 dyn per cm^2$ for both with and without correction. At $\beta_{\perp} = \beta_{\parallel}$ the solution has the same value of growth rate both with correction and without correction, according to Stix [18] this represent the transit time damping which is characterized by isotropic pressure of $P_{\perp} = P_{\parallel}$, which was generated by a sound speed of $C_{\perp} = C_{\parallel}$. The transit-time damping is the magnetic analogue of Landau damping where μB_{\parallel} acts like an electrostatic potential ϕ , where μ is the magnetic moment.

As β_{\perp} decreases below β_{\parallel} , the growth rate began to increase indicating firehose instability. The growth rate reached a value of about $7.49 \times 10^{-6}s^{-1}$ with correction and $5.29 \times 10^{-6}s^{-1}$ without correction for a sound speed of $c_{\perp} = 3.84 \times 10^{-1}cms^{-1}$ and a pressure of $P_{\perp} = 1.62 \times 10^3 dyn per cm^2$. At $\beta_{\parallel} > \beta_{\perp}$ the parallel thermal pressure in the plasma is sufficiently high. The magnetic flux become unstable for transverse oscillations of the magnetic field and at the same time excite parallel propagating Alfvén waves. Therefore as β_{\perp} becomes small for larger β_{\parallel} by a difference of 2, the incompressible fire hose instability sets in as the growth rate increases with decrease in β_{\perp} . The firehose instability is a non-

oscillating, purely growing mode. This result from the parallel thermal pressure in the magnetohydrodynamic fluid being sufficiently high by $P_{\parallel} - P_{\perp} > B^2/\mu_0$, the magnetic flux tubes become unstable for transverse oscillations of the magnetic field and spontaneously excite parallel propagating Alfvén waves. In the magnetohydrodynamic approximation, where these waves are non-dispersive, the wave has no real frequency and is a very-low frequency wave in the lowest part of the Alfvén branch [19].

The firehose instability is a very strong instability, but it requires large parallel pressure or $\beta_{\parallel} > 2$, which implies that the instability is possible only in high-beta or low magnetic field plasmas as, for instance, in the solar wind. This region may therefore become spontaneously excited to release fast growing Alfvén waves with amplitudes which are large. Once excited, the oscillation will propagate as an Alfvén wave along the magnetic field lines into the near-Earth magnetosphere. The physical mechanism of this instability is similar to that which generates oscillations in a water hose when the water pressure exceeds a critical value [4].

As β_{\perp} increases greater than β_{\parallel} , the growth rate began to increase indicating mirror instability. The highest growth rate value obtained for a sound speed of $c_{\perp} = 4.44 \times 10^{-1} \text{ cm s}^{-1}$ and a pressure of $P_{\perp} = 2.14 \times 10^3 \text{ dyn per cm}^2$ are $4.02 \times 10^{-6} \text{ s}^{-1}$ with correction and $2.84 \times 10^{-6} \text{ s}^{-1}$ without correction. Ideally when a compressional wave is set up, it is ordinarily damped out by the transit time damping at $\beta_{\perp} = \beta_{\parallel}$. However, when $\beta_{\perp} > \beta_{\parallel}$, the diamagnetic repulsion of the plasma, which is trapped in the local mirror field created by the wave, excludes the magnetic field. This instability causing a local deformation of the magnetic field makes the plasma spatially inhomogeneous. It occurs because a part of the particles captured in “weak mirror traps” subdivides the distribution of particles into passing and trapped species. This accelerates the flow of plasma into the deepened well of the local mirror, and therefore the perturbation grows as $\beta_{\perp} \gg \beta_{\parallel}$ [4].

Figures 1.2a and 1.2b are the solutions of the test problem which was obtained and plotted. We see that in general the numerical and analytical results agree. The test problem was used as guide to arrive at the solutions in Figures 1.1(a-b). In the test problem, the damping of the growth rate was fast in the fire hose instability curve while in the mirror instability curve the damping was slow compared to that of the solar wind and magnetosphere. This might have resulted due to difference in parameters used for each case.

5.0 Conclusion

We have solved the dispersion relation for the fire hose and mirror growth rates with and without correction using the PDRF for the solar wind. We have found that the results obtained were in accordance with that obtained from previous literature.

We recommend that the kinetic model should be used to solve the dispersion relation. The PDRF code could be used to verify test data from satellites. It could also be used to solve dispersion relation in warm plasma, unmagnetized plasma (by setting $B_0 = 0$).

References

- [1] Bret, A. (2007). Beam plasma dielectric tensor with mathematica, Computer Phys. Comm., 179: 362.
- [2] Swanson, D. G. (2003). Plasma Waves. Second edition, U.S.A.:IOP., (Series in plasma physics).
- [3] Ronnmark, K. (1982). Waves in Homogeneous, Anisotropic, Multi-fluid Plasmas. Kiruna Geophysical Institute Reports, 179.
- [4] Ronnmark, K. (1983). Computation of the dielectric tensor of a Maxwellian plasma. Plasma Phys., 25: 699.
- [5] André, M. (1985). Dispersion surface. J. Plasma Phys., 33 (1): 1-19.
- [6] Xie, H. S. (2013). PDRF: A general dispersion relation solver for magnetized multi-fluid plasmas. Computer Physics Communications, 185: 670 - 675.
- [7] Chew, G. F., Goldberger, M. L. and Low, F. E. (1956). The Boltzmann equation and the one-fluid hydromagnetic equations in the absence of particle collisions. Proc. R. Soc. London, Ser A, 236: 112.
- [8] Li, X., Lewis, H. R., LaBelle, J., Phan, T. D. and Treumann, R. A. (1995). Characteristics of the ion pressure tensor in the earth's magnetosheath. Geophys. Res. Lett., 22: 667- 670.
- [9] Kaufmann, R., Lu, C., Paterson, W. R and Frank, L. A. (2002). Three-dimensional analysis of electric currents and pressure anisotropies in the plasma sheet. J. Geophys. Res., 107 (A7): 1103.
- [10] Hasegawa, A. (1975). Plasma Instabilities and Nonlinear Effects. 1st ed., New York: Springer-Verlag. Vol. 8.
- [11] Kulhánek, P. (2011) *Úvod do teorie plazmatu*. AGA, 1st. edition. In Czech language only.
- [12] Stix, T. (1992). Waves in Plasma. New York: AIP Press.
- [13] Bret, A. and Deutsch, C. (2006). A fluid approach to linear beam plasma electromagnetic instabilities. Phys. Plasmas, 13: 042106.
- [14] Hakim, A. (2008). Towards closures for multi- fluid moment simulations of collisionless plasmas. J. Fusion Energy, 27: 36.
- [15] Goedbloed, J. and Poedts, S. (2004). Principles of Magnetohydrodynamics: With Applications to Laboratory and Astrophysical Plasmas. New York: Cambridge University Press.
- [16] Priest, E. R. and Wood, A. W. (1991). Advances in solar system magnetohydrodynamics. Cambridge university press, Cambridge, New York. P. 368.
- [17] Goldston, R. J. and Rutherford, P. H. (1995). Introduction to plasma physics. Bristol: institute of physics.
- [18] Stix, T. (1962). The theory of plasma waves. New York: McGraw Hill.
- [19] Baumjohann, W. and Treumann, R. A. (1996). Basic Space Plasma Physics. London: Imperial College Press.